NANO LETTERS

Letter

pubs.acs.org/NanoLett

Evolution of the Single-Nanocrystal Photoluminescence Linewidth with Size and Shell: Implications for Exciton–Phonon Coupling and the Optimization of Spectral Linewidths

Jian Cui, Andrew P. Beyler, Igor Coropceanu, Liam Cleary, Thomas R. Avila, Yue Chen, José M. Cordero, S. Leigh Heathcote, Daniel K. Harris, Ou Chen, Jianshu Cao, and Moungi G. Bawendi*

†Department of Chemistry, Massachusetts Institute of Technology, Cambridge, Massachusetts 02139, United States

Supporting Information

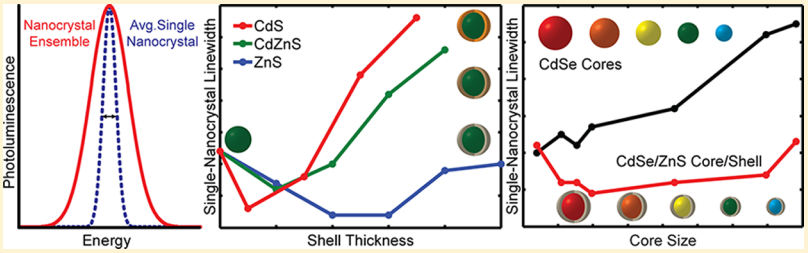

ABSTRACT: The optimization of photoluminescence spectral linewidths in semiconductor nanocrystal preparations involves minimizing both the homogeneous and inhomogeneous contributions to the ensemble spectrum. Although the inhomogeneous contribution can be controlled by eliminating interparticle inhomogeneities, far less is known about how to synthetically control the homogeneous, or single-nanocrystal, spectral linewidth. Here, we use solution photon-correlation Fourier spectroscopy (S-PCFS) to measure how the sample-averaged single-nanocrystal emission linewidth of CdSe core and core/shell nanocrystals change with systematic changes in the size of the cores and the thickness and composition of the shells. We find that the single-nanocrystal linewidth at room temperature is heavily influenced by the nature of the CdSe surface and the epitaxial shell, which have a profound impact on the internal electric fields that affect exciton–phonon coupling. Our results explain the wide variations, both experimental and theoretical, in the magnitude and size dependence in previous reports on exciton–phonon coupling in CdSe nanocrystals. Moreover, our findings offer a general pathway for achieving the narrow spectral linewidths required for many applications of nanocrystals.

KEYWORDS: *semiconductor nanocrystals, colloidal quantum dots, photon-correlation Fourier spectroscopy, spectral linewidth, single-molecule spectroscopy, exciton–phonon coupling, nanoparticle synthesis*

Quantum dots (QDs) are semiconductor materials whose defining feature is that the wave functions of excited electron–hole pairs ("exciton") are confined in all directions by the small spatial dimensions of the particle. As a result, the photophysical properties of these materials are determined not only by their material composition but also by their size and structure. Most strikingly, the energy of the exciton can be tuned simply by changing the particle size.[1]

The chemically synthesized version of quantum dots are colloidal suspensions of crystalline material, that is, nanocrystals or NCs. With advances in synthetic methodology, NCs have been made with high monodispersity,[2] quantum yield,[3] and photostability[4] from the visible[2] to the midwavelength infrared.[5,6] These properties, in addition to their solution-processability and amenability to different types of environments, have made nanocrystals attractive for incorporation into optical applications such as biological imaging,[7] displays,[8] LEDs,[9] lasers,[10,11] photovoltaics,[12,13] solar concentrators,[14,15] and more.[16] Despite the continual improvement of synthetic methods, a property of nanocrystals that has remained elusive to rational design is the emission linewidth. This lack of synthetic control has hindered the performance of many applications, such as displays or biological multiplexing, because they require reproducibly synthesized narrow linewidths for optimal performance.

The ensemble photoluminescence spectrum of a sample of nanocrystals is defined by the convolution of the average emission spectrum of the individual particles (homogeneous broadening) and the distribution of emission wavelengths of the particles in the sample (inhomogeneous broadening) (Figure 1). Many synthetic methods have sought to achieve narrow spectral linewidths by eliminating interparticle polydispersity. In fact, our group has demonstrated that CdSe/CdS core/shell nanocrystals can be synthesized with near-perfect chromatic homogeneity.[4] However, this approach addresses only one of the factors that determine the overall ensemble

Received: September 18, 2015
Revised: November 29, 2015
Published: December 4, 2015

DOI: 10.1021/acs.nanolett.5b03790
Nano Lett. 2016, 16, 289–296

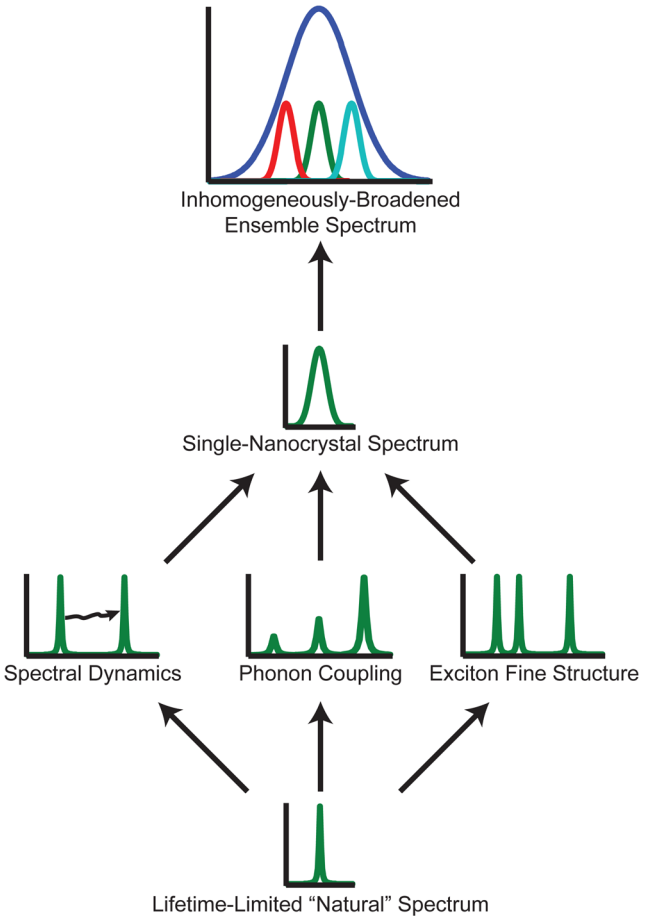

Figure 1. An ensemble spectrum consists of the intrinsic single-emitter spectrum convolved with the interparticle inhomogeneities. The single-emitter spectrum arises from a combination of exciton−phonon coupling of the lifetime-limited "natural" spectrum, spectral dynamics, and emission from fine-structure states.

emission linewidth. Even the most monodisperse of samples will not have a narrow spectral linewidth if the spectra of the individual particles is inherently broad. Further efforts to maximize the utility of nanocrystals for optical applications must address the synthetic control of the single-emitter contribution to the spectral linewidth.

The single-nanocrystal spectrum is understood to originate from broadening of the lifetime-limited "natural" spectrum through interactions of the exciton with its environment.[17] In Figure 1, we highlight several of the key spectral-broadening mechanisms found in single nanocrystals. Spectral diffusion is a phenomenon that is commonly observed at cryogenic temperatures. Typically photoinduced, fluctuations in local electric fields due to migrating charges can lead to spectral shifts due to the Stark effect.[18−20] At room temperature, however, spectral diffusion has been found to be negligible on submillisecond time scales in CdSe core/shell nanocrystals.[21]

Excitonic coupling to phonons within the nanocrystal serves to dephase any given electronic transition and to produce phonon sidebands, where emission is energetically displaced from the zero-phonon transition. These interactions, which can occur via various mechanisms with different types of phonons, have been the topic of numerous conflicting reports on both the coupling strength and dependence with nanoparticle size.[22−27]

Further complicating matters is that the ground-state exciton in nanocrystals can consist of multiple electronic fine-structure states, several of which are optically active.[28] Depending on the energy differences between fine-structure states and the temperature of the system, emission can originate from multiple electronic states, each with its own phonon coupling properties. Understanding the interplay of these mechanisms in single nanocrystals is not only integral to our fundamental understanding of excitonic emission, but also to the synthesis of nanostructures with narrow spectral linewidths.

Ideally, the single-nanocrystal contribution to the ensemble spectrum can be experimentally determined by spatially separating the particles and studying the photoluminescence spectra of individual particles one at a time.[20,29,30] However, because of heterogeneity between particles within a sample batch, it can be difficult to ascribe properties measured from single nanocrystals to the entire sample and, more importantly, to changes in chemical synthesis. The process of building ensemble statistics from individual particles is tedious, prone to selection bias, and susceptible to artifacts such as photodegradation or unwanted interactions with the environment. A more robust and reliable method for establishing the link between synthesis and single-nanocrystal spectra is solution photon-correlation Fourier spectroscopy (S-PCFS).

Rather than measuring the spectrum of one nanoparticle at a time as in traditional single-particle photoluminescence spectroscopy, S-PCFS parses the photon stream from nanocrystals diffusing through a laser focal volume into photon pairs from the same emitter and photon pairs from different emitters.[31,32] With this approach, we can probe the spectral information of single nanocrystals in their native environment at fast time scales with short exposure times, without user selection bias, and with ensemble-level statistics. S-PCFS has proven to be a reliable and robust probe of spectral dynamics (or the lack thereof)[21] as well as spectral homogeneity and inhomogeneity in nanocrystals at room temperature.[32,33]

S-PCFS measures the spectral correlation function $p^{\text{single}}(\zeta, \tau)$ for the average single emitter in an ensemble, where ζ is the energy difference and τ is the temporal spacing between photon pairs.[32,34] An *effective* spectral line shape (ESL) is then inferred from the spectral correlation. In the case of nanocrystals at room temperature, the underlying spectrum can be approximated as a superposition of Gaussian functions because the spectrum is singly peaked and nearly symmetric. The full-width at half-maximum of this effective spectral line shape is taken to be the "single-nanocrystal linewidth" averaged over the entire sample.[33]

In this work, we explore the single-NC linewidth of CdSe particles with systematic differences in size, shell thickness, and shell composition. Our results indicate that a major contribution to the single-NC linewidth is coupling to longitudinal optical (LO) phonons. These couplings are highly dependent on the nature of the CdSe surface and shell because of the sensitivity of the Fröhlich coupling mechanism to internal electric fields. The ground-state exciton fine structure is also believed to contribute a small but non-negligible component to the single-NC linewidth. From these considerations, we lay down a pathway towards the rational optimization of single-NC linewidths through chemical synthesis.

We first test our understanding of the fundamental physics of the spectral linewidth in nanocrystals by investigating the defining feature of quantum-confined systems: the dependence

DOI: 10.1021/acs.nanolett.5b03790
Nano Lett. 2016, 16, 289−296

on size. As we show below, the precise nature of the nanocrystal surface plays a significant role in the width of the single-NC spectrum. With this complexity in mind, we performed two sets of syntheses to ensure consistency in our synthetic procedure. For the first set of CdSe cores, we drew aliquots from the flask as CdSe cores grew following a hot injection. In the second set, we performed the same procedure but for multiple batches of CdSe cores.

As can be clearly seen in Figure 2, the single-NC linewidth decreases nearly monotonically with increasing particle size.

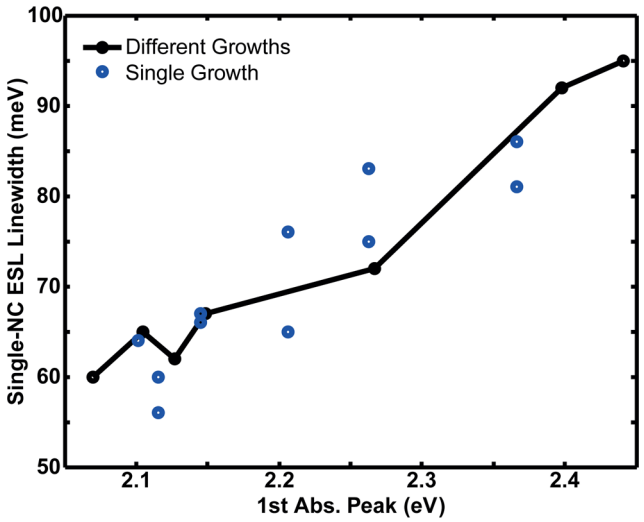

Figure 2. Effective single-NC spectral linewidths measured from S-PCFS are plotted for CdSe cores of different sizes drawn from a single synthesis batch and from multiple batches. For the single-batch growth, we plot the single-NC linewidth values for two separate S-PCFS measurements. In both cases, the single-NC linewidth decreases nearly monotonically as a function of the nanocrystal size.

This is the case for aliquots drawn from a single synthetic batch and from different batches. The quantitative linewidth values are in good agreement between the two sets of measurements, indicating consistency in experimental execution of both synthesis and spectroscopy. It is evident from this result that for CdSe cores, the single-NC linewidth decreases significantly and nearly monotonically as the particle size increases.

This result has two implications. First, though classical nucleation theories predict size focusing during particle growth, the attribution of size focusing to a given synthesis cannot be made purely on the basis of the width of the ensemble spectrum.[35] Figure 2 shows that the ensemble spectrum will narrow with core growth even without size focusing. Second, this result provides a peek into which sources of homogeneous broadening (Figure 1), exciton−phonon coupling or fine-structure emission, make major contributions to the average linewidth that we observe.

The ground-state exciton in CdSe nanocrystals is understood to be 8-fold degenerate in the particle-in-a-sphere approximation.[28,36] These electronic states are split into optically active ("bright") and optically inactive ("dark") states once the size, shape, and crystal structure of the particle are taken into account. Because the energy splitting between bright fine-structure states is often calculated to be less than the thermal energy k_BT,[36,37] the room-temperature single-NC emission spectrum is expected to have some contribution from multiple states.

In the case of Figure 2, such a large change in spectral linewidth cannot be explained solely by a change in the fine-structure energy splittings. A simple calculation of offset Gaussian functions weighted by the Boltzmann factor shows that the exciton fine structure should not contribute more than ∼8 meV to linewidth changes (see Supporting Information). Thus, the linewidth narrowing with increasing size must be due primarily to a decrease in exciton−phonon coupling.

In principle, the single-NC emission spectrum should clearly reflect exciton−phonon coupling in the system. However, room-temperature spectra are broad and often featureless, making it difficult to determine the contributions of specific phonons and the mechanisms involved. Rather than analyzing the spectrum of a single sample, we alter parameters such as the nanocrystal size, shell and composition to better understand the spectral-broadening mechanisms involved. We will show with these measurements that the decreasing exciton−phonon coupling with increasing CdSe core size in Figure 2 is not an intrinsic effect due to quantum confinement, but rather an extrinsic surface-related effect.

In our previous study, we observed that the single-NC linewidth of core/shell nanocrystals can show great variability between different synthetic batches with a strong dependence on the shell.[33] In a particularly striking example, we observed that CdS shell growth leads to significant broadening of the single-NC linewidth. To determine the role of the shell on the sample-averaged single-particle spectral linewidth, we compared three different shell compositions grown on the same cores. A single batch of CdSe cores was split for three different overcoatings performed under nearly identical conditions with similar organometallic precursors: ZnS, CdS, and CdZnS (50% Cd, 50% Zn). Aliquots were drawn during shell growth at points that roughly correspond to the expected number of shell monolayers. Figure 3 shows that in each case, the single-NC linewidth first decreases upon shell growth with a subsequent linewidth broadening with further shell growth. However, the progression of the single-NC linewidth broadening depends on the composition of the shell. Both the linewidth narrowing and

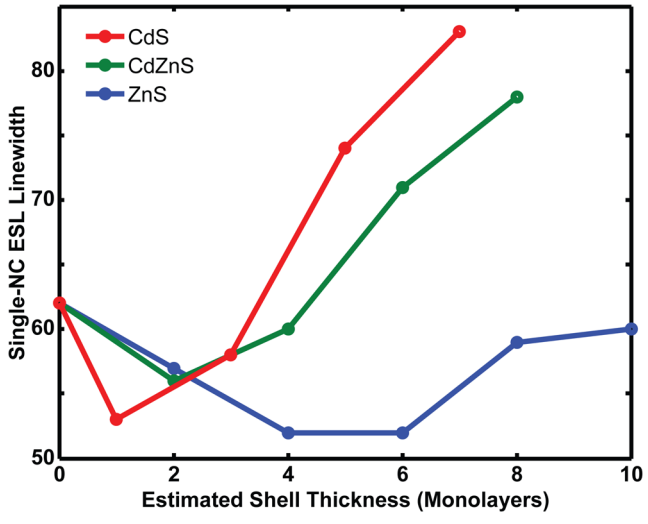

Figure 3. Effective single-nanocrystal linewidths are plotted for different shell thicknesses of three different compositions grown on the same batch of CdSe cores. For each sample, the single-NC linewidth initially narrows with shell growth then broadens again.

DOI: 10.1021/acs.nanolett.5b03790
Nano Lett. 2016, 16, 289−296

broadening suggest that LO−phonon coupling is the predominant mechanism involved.

All three samples exhibit an unexpected narrowing of the spectrum with initial shell growth that suggests that an extrinsic surface effect is at play (Figure 3). The observed reduction in single-NC linewidth is consistent with passivation of trap states on the surface of the CdSe particles.[38,39] A reduction in trapped surface charges also reduces excitonic coupling to the LO phonon as the presence of a localized surface charge induces a polarization in the nanocrystal, enhancing LO−phonon coupling.[24,40,41] In fact, the presence of an extra charge within a CdSe quantum dot has been predicted to increase LO−phonon coupling by nearly 2 orders of magnitude due to changes in the electron−hole wave function overlap.[42] Our observation, corroborated by prior measurements using resonance Raman spectroscopy,[43−45] is a strong indication that the single-NC linewidth is sensitive to LO phonon coupling. We note that each of these resonance Raman reports observed reductions in CdSe LO−phonon coupling with shell growth despite measurements on slightly different core/shell nanocrystals, in support of a general mechanism in nanocrystals, such as passivating surface charges. Most importantly, however, this observation shows that bare CdSe cores are not appropriate for studies of exciton−phonon coupling because of the significant influence of trapped charges.

Although the narrowing of the single-NC linewidth with shell growth can be explained by an extrinsic effect, the subsequent broadening with increasing shell thickness reflects an intrinsic property of the shell. In the case of ZnS shell growth, we measure little-to-no broadening of the single-NC linewidth. In contrast, the CdS and CdZnS shell growth lead to significant linewidth broadening, in accordance with what was observed in ref 33. We emphasize that this broadening occurs despite having used a different CdS overcoating protocol in ref 33, suggesting that it is an intrinsic effect. As in the case of Figure 2, the very large linewidth changes observed for the CdZnS and CdS shell growths cannot be due solely to changes in the exciton fine structure. This dramatic linewidth broadening is consistent with an increased Fröhlich interaction due to a decrease in the wave function overlap between the electron and hole wave functions and stronger coupling to phonons in the shell.

CdSe/ZnS core/shell particles are believed to be Type-I heterostructures. That is, the electron and hole are largely confined to the core. On the other hand, CdSe/CdS core/shell particles are often quasi-Type II heterostructures, where the electron wave function leaks into the CdS shell, but the hole remains confined in the CdSe core.[46] As the CdS shell grows, the overlap between the electron and hole wave functions decreases, inducing an increasingly large polarization in the nanocrystal that enhances coupling to LO phonons. In studies of other nanostructures, this effect can be extremely large.[47] Additionally, the exciton can couple to phonons of the shell material as the charge carrier wave functions delocalize into the shell.[48,49] The fact that Fröhlich coupling is the dominant phonon-coupling mechanism in CdS[50] further suggests that coupling to the shell phonons plays a significant role in the broadening[51] in addition to changes in wave function overlap.

The linewidth broadening that is observed with very thick ZnS shells may arise from a combination of several different mechanisms. In an effort to disentangle these different mechanisms, the same CdSe cores that were measured in Figure 2 were used for ZnS overcoating. The overcoating method was similar to that used for the samples in Figure 3.

In Figure 4a, we show the evolution of the single-NC linewidth for CdSe cores of different sizes with different

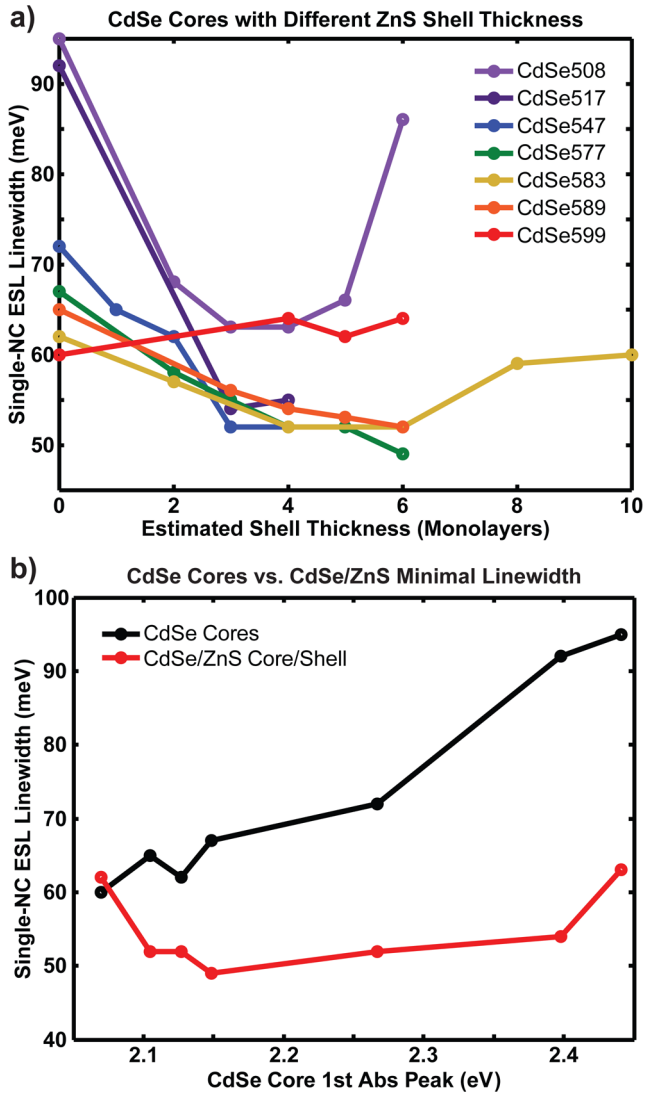

Figure 4. (a) Single-NC spectral linewidths are shown for several sizes of CdSe cores with increasing thickness of a ZnS shell. (b) Single-NC spectral linewidths are shown for CdSe cores (black, reproduced from Figure 2). The narrowest of the single-NC linewidths measured for different shell thicknesses in (a) are plotted as a function of the core size (red).

thicknesses of a ZnS shell. For nearly every size, the single-NC linewidth initially decreases with ZnS shell growth, as discussed with regards to Figure 3, signifying a reduction in exciton−phonon coupling due to surface passivation. The linewidth then plateaus after several monolayers. For some core sizes, we measured a subsequent increase in the single-NC linewidth with increasing ZnS growth, as in Figure 3.

Because of the large lattice mismatch between CdSe and ZnS, shell growth imparts considerable strain on the nanoparticle.[48] With increased shell growth, additional strain is placed onto the surface of the cores, forcing reconstruction and relaxation into a distorted lattice with an increased likelihood of defect site formation.[39] The increase in single-NC linewidth

DOI: 10.1021/acs.nanolett.5b03790
Nano Lett. 2016, 16, 289−296

with very thick ZnS shell growth can be attributed to either the creation of new trap sites by surface reconstruction or increased electric fields within the nanoparticle due to the piezoelectric effect.[52] The dramatic decrease and increase of the single-NC linewidth in the smallest nanocrystals may be indicative of the fact that smaller nanocrystals are more strained and undergo more substantial reconstruction.[53−55]

Despite all of the complexity, the data in Figure 4a suggest that growth of a ZnS shell on CdSe cores eliminates some of the extrinsic sources of enhanced exciton−phonon coupling. In light of this, we examined the narrowest measured linewidths for different sizes of CdSe cores and thicknesses of ZnS shell. In Figure 4b, we plot the single-NC linewidth values for CdSe cores (reproduced from Figure 2) against the minimal single-NC linewidth values for the same cores with ZnS shell. Although CdSe cores exhibit a strong size dependence of the single-NC linewidth, the minimal single-NC linewidth is effectively constant (given the error in the measurements as seen in Figure 2) over nearly the entire range of sizes for CdSe/ZnS core/shell particles. This is in agreement with recent reports using resonance Raman spectroscopy.[27,45]

The lack of size dependence in CdSe/ZnS core/shell particles is again likely due to LO phonon coupling. In this "strong confinement" regime, both the electron and hole wave functions are confined by the spatial dimensions of the particle.[42,56] In this regime, the spatial overlap of the wave functions is very high and thus, there is little change in the LO phonon coupling with size. There appears to be a slight increase in the single-NC linewidth with the smallest particle, but as mentioned before, this may have more to do with the surface strain in such small particles than a confinement-related effect. For larger particles, the increase in single-NC linewidth may reflect a decrease in the overlap between the electron and hole wave functions. Ref 56 has measured the change in wave function localization within CdSe cores and found that when the particle size is larger than a critical size, the hole wave function is no longer extended throughout the entire nanocrystal. Beyond this size, we would expect increased LO−phonon coupling with increasing size as the overlap with the electron wave function decreases.

We note that some of these single-NC linewidth changes may be affected slightly by the exciton fine structure. The exciton fine structure is significantly affected not only by the size of the particles, but the aspect ratio as well.[57,58] In addition, ZnS shell growth often occurs with a preferential orientation.[59] Without knowing the precise size and shape of the nanocrystals during shell growth, the effect of the fine structure on the single-NC linewidth is unclear. Nevertheless, it is possible that small changes, such as the reddest dots with ZnS growth (Figure 4a) or the increase in single-NC linewidth for the largest core sizes (Figure 4b), may arise from an increase in fine-structure splitting. Our current data cannot unambiguously distinguish whether a change in fine structure or phonon coupling is the dominant contribution here. We discuss below further work that could be performed to disentangle the different contributions from each mechanism.

Our results indicate that the single-NC linewidth is a strong function of the LO−phonon coupling in the nanocrystal. There are essentially two types of phonons in nanocrystals that couple to the exciton: low-energy acoustic phonons and higher-energy optical phonons.[22,23] Phonon coupling to the exciton occurs through a nonpolar deformation potential interaction or a polar interaction (piezoelectric coupling for acoustic phonons and Frölich coupling for optical phonons). The addition of a thin shell (Figures 3 and 4a) is unlikely to dramatically change the way phonons deform the lattice, therefore suggesting a polar interaction at play. Among the polar interactions, piezoelectric coupling to acoustic phonons is expected to be negligible in small nanocrystals,[60] but our data show that the linewidth change with shell is significant for the smallest nanocrystals. What is clear, however, is that a thin shell layer can dramatically reduce trapped charges,[38,39] which are understood to significantly affect LO−phonon coupling.[24,40−42] Resonance Raman experiments[43−45] support our conclusion that LO−phonon coupling is responsible for these single-NC linewidth changes. The subsequent linewidth broadening with shell thickness, that is highly dependent on the CdS content of the shell (Figure 3), additionally support the significance of LO−phonon coupling in single-NC linewidth broadening.

The specific nature of the surface appears to strongly dictate the exciton−phonon coupling. For instance, the dependence of the single-NC linewidth on particle size is vastly different for bare CdSe cores than for CdSe/ZnS core/shell particles. The data suggest that trapped surface charges affect the internal fields more for smaller particle sizes simply because of proximity.[18] In the case of core/shell particles, where these surface charges are eliminated (Figure 4b), a different trend is revealed. We also observe changes in the single-NC linewidth that suggest that surface strain, surface reconstruction, and the nature of the core/shell interface affect the exciton−phonon coupling.

Once we recognize that the crystalline nature of the nanoparticle surface plays a role in exciton−phonon coupling, it is easy to see the limitations of previous theoretical studies on this subject. A consideration of nanocrystals that would be absent in a simple spherical quantum dot model is the internal dipole moment. The ground-state dipole moment of the nanocrystal, which is understood to be primarily along the *c* axis of the wurtzite crystal, is enhanced because of the presence of polar facets at the ends of this axis.[59,61−63] Moreover, the dipole moment is heavily affected by surface reconstruction and stoichiometry.[62,64] Changes in this ground-state dipole affect the internal electric fields that govern LO−phonon coupling and must be taken into consideration when studying exciton−phonon coupling. Early theoretical works that predicted extremely small LO−phonon couplings[42] in quantum dots did not consider the fact that the internal dipole could be so strong nor did they consider that the surface of the nanocrystal would influence the internal electric fields so significantly. We note that this concept was hypothesized to affect LO−phonon coupling in nanocrystals at least as far back as 1996 in a review paper which stated, "...other effects, such as the presence of polar crystallographic faces, may act to separate the optically generated electron−hole pair...".[65]

Others in the literature have noted the connection between LO−phonon coupling and local electric fields. In ref 18, spectral shifts at low temperature were understood to occur due to changes in the local electric fields that induced Stark shifts and were correlated with LO−phonon coupling. Single CdSe core/shell particles at room temperature were found to exhibit a similar correlation between spectral linewidth and spectral position.[66,67] In these works, the correlation between spectral position and linewidth were considered in the context of rapid spectral diffusion. However, we have previously established that rapid spectral diffusion is negligible at room temperature.[21] Our new results suggest that the linewidth variations measured in

DOI: 10.1021/acs.nanolett.5b03790
Nano Lett. 2016, 16, 289−296

single nanocrystals are instead a result of changes in exciton−phonon coupling, perhaps due to charges on the surface or perhaps simply due to differences in the surface structure of dots, altering the internal electric fields. A tool such as S-PCFS, which can measure single-NC spectral properties over an entire sample batch, was necessary to make this connection because the properties of individual particles can be so varied.

Consideration of the permanent dipole of nanocrystals has a profound impact on the optimization of spectral linewidths nanocrystals of different compositions. One may expect that nanocrystals with crystal structures lacking a spontaneous polarization, such as zincblende or rock salt, would not have permanent dipole moments. However, due to the imperfections in nanoparticle growth, polar facets often result and dipole moments can exist.[68] Measurements on zincblende CdSe core/shell particles indicate that they have similar single-NC spectral linewidths as their wurtzite counterpart (see Supporting Information). Moreover, these considerations should hold for the lead chalcogenide particles as well. Despite predictions that LO−phonon coupling should be extremely weak in these particles,[40,41] truncation of the structure and asymmetry in the orientation of polar facets result in strong internal dipoles that can lead to strong exciton−phonon couplings, as in CdSe.[69] This may be the mechanism responsible for the broad spectra observed in single PbS nanocrystals.[70] S-PCFS studies performed on these lead chalcogenide particles would confirm the breadth of the single-NC linewidth.

Efforts to precisely determine the size dependence of exciton−phonon coupling in nanocrystals are stymied by the fact that a confluence of factors such as localized charges, surface reconstruction, and the piezoelectric effect contribute to changes in the local electric fields that govern LO−phonon coupling. We suspect that differences in sample preparation that were unable to normalize for all of these effects may have been at the root of experimental discrepancies regarding exciton−phonon coupling in the literature.[22,23] Moreover, determining the size dependence of exciton−phonon coupling in colloidal quantum dots may not even be a meaningful endeavor since the crystalline nature of these nanoparticles prevents such categorization.

Though exciton−phonon coupling appears to be the dominant source for the single-NC linewidth variations that we have observed, emission from multiple fine-structure states is expected have a non-negligible contribution to the spectral breadth (see Supporting Information). Unfortunately, efforts to determine the precise contribution of the fine structure are complicated by the fact that fine-structure splittings are sensitive to both the size and shape of the particle.[57,58,71,72] A Herculean effort appears to be in order to determine the precise effects of the fine structure. Temperature-dependent S-PCFS studies must be performed on core/shell particles of different sizes, shell thicknesses, and aspect ratios. Detailed structural studies and spectral lineshape modeling must then complement the spectroscopic measurements to provide a clear picture.

We can estimate the contribution of the exciton fine structure to the single-NC linewidth by calculating the bright-state energy splittings[36] scaled by the Boltzmann factor. For small splittings, the fine-structure contribution to the linewidth is approximately the energy separation itself. For large splittings, the energy splitting should not contribute to any broadening. We plot in Figure 5 the larger of the Boltzmann-weighted energy splittings between the three bright fine-structure levels as a function of size and ellipticity for CdSe nanocrystals. This calculation shows that the narrowest single-NC linewidths are achieved for certain aspect ratios where the fine structure contributes the least to linewidth broadening. Most strikingly, particularly for the larger nanocrystals, the optimal aspect ratio is an elongated particle. This is in agreement with the observation in ref 33 that the sample with the narrowest single-NC linewidth contained elongated core/shell particles.

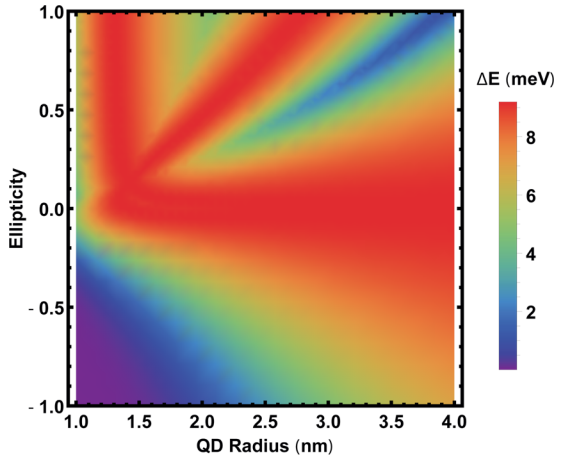

Figure 5. Heatmap of the estimated contribution of fine-structure states to the spectral linewidth as a function of the particle size and aspect ratio. It is calculated as the maximum energy separation between bright fine-structure states scaled by the Boltzmann factor ($\Delta E = dE \cdot e^{-dE/k_BT}$, where dE is the energy difference and k_BT is the available thermal energy). The y axis corresponds to the ellipticity, c, of the dot (defined by $a/b = 1+ c$, where a and b are the major and minor axes, respectively), whereas the x axis is the radius of the quantum dot.

We leave the reader with several design principles for optimizing the spectral breadth of the nanocrystal emission. First, the particles must be made as monodisperse as possible. Second, the particles should have surfaces that are perfectly passivated, relaxed, and balanced in their stoichiometry. Passivation eliminates surface traps that broaden the spectrum and surface relaxation, reconstruction, and stoichiometry minimize the internal dipole. For core/shell particles, the shell material should have no lattice mismatch with the core. Finally, the particles should be at the perfect aspect ratio such that for any given size, the exciton fine structure contributes as little as possible to the single-NC linewidth.

The ultimate limit of our design principles is illustrated in CdSe colloidal nanoplatelets, which have the narrowest linewidths observed in semiconductor nanostructures.[73] First, inhomogeneous broadening does not exist because the nanoparticle surface orthogonal to the confinement direction is atomically perfect.[74] Additionally, these surfaces are relaxed with no further reconstruction necessary, thereby minimizing the internal dipole. Combined with the fact that wave function overlap is maximized in the confinement dimension because the particles are only a few monolayers thick, these particles have extremely low LO−phonon coupling.[75] Lastly, the splitting between the light-hole and heavy-hole transitions is so large that upper bright states cannot contribute to the emission spectrum.[76] As shown in Figure 6, the spectral correlation for an ensemble of CdSe nanoplatelets is narrower than the single-particle spectral correlation measured using S-PCFS for colloidal quantum dots of similar emission energy.

DOI: 10.1021/acs.nanolett.5b03790
Nano Lett. 2016, 16, 289−296

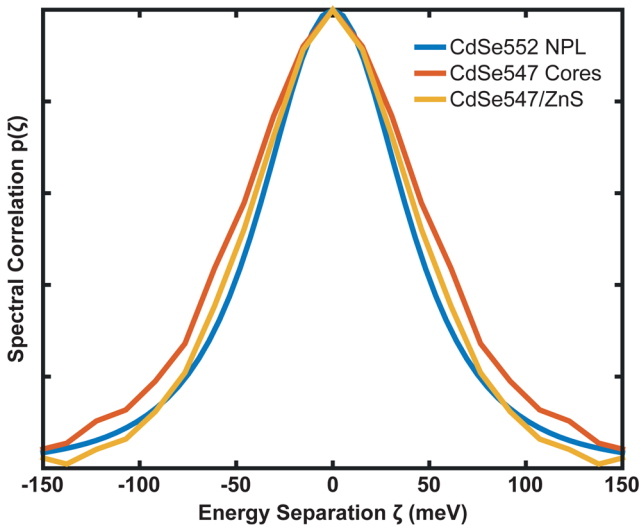

Figure 6. Spectral correlation of the ensemble spectrum of five-monolayer CdSe nanoplatelets is compared with the single-NC spectral correlations, measured using S-PCFS, of core and core/shell CdSe quantum dots of similar absorption wavelength of similar absorption wavelength.

Finally, we note that colloidal nanoplatelets of CdS have been synthesized[76] with significantly broader emission spectra than their CdSe counterparts.[51] Additionally, these CdS nanoplatelets have noticeably large Stokes shifts while CdSe nanoplatelets have essentially no Stokes shifts. Combining the fact that CdS has strong LO−phonon coupling[50] with the knowledge that the Stokes shift is typically an indication of net exciton−phonon coupling[23] further reinforces the importance of LO−phonon coupling to the breadth of single nanostructures.[51]

In this work, we have used Solution-PCFS to study the single-nanocrystal emission linewidth of particles of varying size, shell composition, and shell thickness. From these measurements, we have considered the importance of various mechanisms responsible for broadening the single-NC linewidth. In particular, LO−phonon coupling and fine-structure splittings have the most dramatic effect on linewidth broadening and can be controlled by altering the nature of the nanoparticle surface and the aspect ratio of the particle. With this knowledge, we have outlined several general design principles for the rational optimization of emission linewidths for emissive semiconductor nanostructures as a whole.

Methods. Details of the S-PCFS setup and analysis used in this work can be found in ref 33 and its Supporting Information. Conceptual and theoretical understanding of the S-PCFS technique can also be found in refs 21, 31, and 32.

■ ASSOCIATED CONTENT

Supporting Information

The Supporting Information is available free of charge on the ACS Publications website at DOI: 10.1021/acs.nanolett.5b03790.

Details of the nanoparticle synthesis, a simple calculation of the effect of fine-structure states on spectra, and a comparison of wurtzite and zincblende QDs. (PDF)

■ AUTHOR INFORMATION

Corresponding Author

*E-mail: mgb@mit.edu. Phone: 617-253-9796.

Author Contributions

J. Cui and M.G.B. conceived of the study. J. Cui performed S-PCFS. Y.C., S.L.H., D.K.H., and O.C. performed CdSe core synthesis. J. Cui, J.M.C., and S.L.H. performed CdSe overcoating. I.C. and A.P.B. performed calculations of the effects of the exciton fine structure. J.C., A.P.B., I.C., L.C., and T.R.A. analyzed data with guidance from J. Cao and M.G.B. J. Cui wrote the manuscript with input from all authors.

Notes

The authors declare no competing financial interest.

■ ACKNOWLEDGMENTS

This work was primarily supported by the United States Department of Energy, Office of Basic Energy Sciences, Division of Materials Sciences and Engineering (Award No. DE-FG02-07ER46454). This work also received support from the National Institutes of Health (5-U54-CA151884-05) and the Army Research Office through the Institute for Soldier Nanotechnologies (W911NF-13-D-0001). L.C. and T.R.A. of the Cao group were supported by the National Science Foundation (Grant No. CHE-1112825) and the Center for Excitonics, an Energy Frontier Research Center funded by the U.S. Department of Energy, Office of Science, Basic Energy Sciences under Award No. DE-SC0001088. J.C., D.K.H., and I.C. gratefully acknowledge support from the National Science Foundation Graduate Research Fellowship Program. The authors thank Igor Fedin, Chunxing She, and Dmitri Talapin for providing the CdSe nanoplatelets.

■ REFERENCES

(1) Bawendi, M. G.; Steigerwald, M. L.; Brus, L. E. *Annu. Rev. Phys. Chem.* **1990**, *41*, 477−496.
(2) Murray, C. B.; Norris, D. J.; Bawendi, M. G. *J. Am. Chem. Soc.* **1993**, *115*, 8706−8715.
(3) Greytak, A. B.; Allen, P. M.; Liu, W.; Zhao, J.; Young, E. R.; Popovic, Z.; Walker, B. J.; Nocera, D. G.; Bawendi, M. G. *Chem. Sci.* **2012**, *3*, 2028−2034.
(4) Chen, O.; Zhao, J.; Chauhan, V. P.; Cui, J.; Wong, C.; Harris, D. K.; Wei, H.; Han, H.-S.; Fukumura, D.; Jain, R. K.; Bawendi, M. G. *Nat. Mater.* **2013**, *12*, 445−451.
(5) Zimmer, J. P.; Kim, S.-W.; Ohnishi, S.; Tanaka, E.; Frangioni, J. V.; Bawendi, M. G. *J. Am. Chem. Soc.* **2006**, *128*, 2526−2527.
(6) Lhuillier, E.; Keuleyan, S.; Liu, H.; Guyot-Sionnest, P. *Chem. Mater.* **2013**, *25*, 1272−1282.
(7) Medintz, I. L.; Uyeda, H. T.; Goldman, E. R.; Mattoussi, H. *Nat. Mater.* **2005**, *4*, 435−446.
(8) Kim, T.-H.; Cho, K.-S.; Lee, E. K.; Lee, S. J.; Chae, J.; Kim, J. W.; Kim, D. H.; Kwon, J.-Y.; Amaratunga, G.; Lee, S. Y.; Choi, B. L.; Kuk, Y.; Kim, J. M.; Kim, K. *Nat. Photonics* **2011**, *5*, 176−182.
(9) Shirasaki, Y.; Supran, G. J.; Bawendi, M. G.; Bulović, V. *Nat. Photonics* **2012**, *7*, 13−23.
(10) Eisler, H.-J.; Sundar, V. C.; Bawendi, M. G.; Walsh, M.; Smith, H. I.; Klimov, V. *Appl. Phys. Lett.* **2002**, *80*, 4614−4616.
(11) Dang, C.; Lee, J.; Breen, C.; Steckel, J. S.; Coe-Sullivan, S.; Nurmikko, A. *Nat. Nanotechnol.* **2012**, *7*, 335−339.
(12) Tang, J.; Sargent, E. H. *Adv. Mater.* **2011**, *23*, 12−29.
(13) Chuang, C.-H. M.; Brown, P. R.; Bulović, V.; Bawendi, M. G. *Nat. Mater.* **2014**, *13*, 796−801.
(14) Coropceanu, I.; Bawendi, M. G. *Nano Lett.* **2014**, *14*, 4097−4101.

DOI: 10.1021/acs.nanolett.5b03790
Nano Lett. 2016, 16, 289−296

(15) Meinardi, F.; Colombo, A.; Velizhanin, K. A.; Simonutti, R.; Lorenzon, M.; Beverina, L.; Viswanatha, R.; Klimov, V. I.; Brovelli, S. *Nat. Photonics* **2014**, *8*, 392−399.
(16) Talapin, D. V.; Lee, J.-S.; Kovalenko, M. V.; Shevchenko, E. V. *Chem. Rev.* **2010**, *110*, 389−458.
(17) Nguyen, D.; Voisin, C.; Roussignol, Ph.; Roquelet, C.; Lauret, J.; Cassabois, G. *Chem. Phys.* **2013**, *413*, 102−111.
(18) Empedocles, S. A.; Bawendi, M. G. *Science* **1997**, *278*, 2114−2117.
(19) Empedocles, S. A.; Bawendi, M. G. *J. Phys. Chem. B* **1999**, *103*, 1826−1830.
(20) Empedocles, S. A.; Neuhauser, R.; Shimizu, K.; Bawendi, M. G. *Adv. Mater.* **1999**, *11*, 1243−1256.
(21) Marshall, L. F.; Cui, J.; Brokmann, X.; Bawendi, M. G. *Phys. Rev. Lett.* **2010**, *105*, 053005.
(22) Kelley, A. M. *J. Phys. Chem. Lett.* **2010**, *1*, 1296−1300.
(23) Kelley, A. M. *ACS Nano* **2011**, *5*, 5254−5262.
(24) Sagar, D. M.; Cooney, R. R.; Sewall, S. L.; Dias, E. A.; Barsan, M. M.; Butler, I. S.; Kambhampati, P. *Phys. Rev. B: Condens. Matter Mater. Phys.* **2008**, *77*, 235321.
(25) Salvador, M. R.; Hines, M. A.; Scholes, G. D. *J. Chem. Phys.* **2003**, *118*, 9380−9388.
(26) Salvador, M. R.; Graham, M. W.; Scholes, G. D. *J. Chem. Phys.* **2006**, *125*, 184709.
(27) Lin, C.; Gong, K.; Kelley, D. F.; Kelley, A. M. *J. Phys. Chem. C* **2015**, *119*, 7491−7498.
(28) Efros, Al. L.; Rosen, M. *Annu. Rev. Mater. Sci.* **2000**, *30*, 475−521.
(29) Moerner, W. E.; Orrit, M. *Science* **1999**, *283*, 1670−1676.
(30) Moerner, W. E.; Fromm, D. P. *Rev. Sci. Instrum.* **2003**, *74*, 3597−3619.
(31) Brokmann, X.; Marshall, L. F.; Bawendi, M. G. *Opt. Express* **2009**, *17*, 4509−4517.
(32) Cui, J.; Beyler, A. P.; Bischof, T. S.; Wilson, M. W. B.; Bawendi, M. G. *Chem. Soc. Rev.* **2014**, *43*, 1287−1310.
(33) Cui, J.; Beyler, A. P.; Marshall, L. F.; Chen, O.; Harris, D. K.; Wanger, D. D.; Brokmann, X.; Bawendi, M. G. *Nat. Chem.* **2013**, *5*, 602−606.
(34) Brokmann, X.; Bawendi, M. G.; Coolen, L.; Hermier, J.-P. *Opt. Express* **2006**, *14*, 6333−6341.
(35) Peng, X.; Wickham, J.; Alivisatos, A. *J. Am. Chem. Soc.* **1998**, *120*, 5343−5344.
(36) Efros, Al. L.; Rosen, M.; Kuno, M.; Nirmal, M.; Norris, D. J.; Bawendi, M. *Phys. Rev. B: Condens. Matter Mater. Phys.* **1996**, *54*, 4843−4856.
(37) Moreels, I.; Raino, G.; Gomes, R.; Hens, Z.; Stoferle, T.; Mahrt, R. F. *ACS Nano* **2011**, *5*, 8033−8039.
(38) Hines, M. A.; Guyot-Sionnest, P. *J. Phys. Chem.* **1996**, *100*, 468−471.
(39) Dabbousi, B. O.; Rodriguez-Viejo, J.; Mikulec, F. V.; Heine, J. R.; Mattoussi, H.; Ober, R.; Jensen, K. F.; Bawendi, M. G. *J. Phys. Chem. B* **1997**, *101*, 9463−9475.
(40) Krauss, T. D.; Wise, F. W. *Phys. Rev. B: Condens. Matter Mater. Phys.* **1997**, *55*, 9860.
(41) Wise, F. W. *Acc. Chem. Res.* **2000**, *33*, 773−780.
(42) Nomura, S.; Kobayashi, T. *Phys. Rev. B: Condens. Matter Mater. Phys.* **1992**, *45*, 1305.
(43) Dzhagan, V.; Valakh, M. Y.; Raevska, O.; Stroyuk, O.; Kuchmiy, S. Y.; Zahn, D. *Nanotechnology* **2009**, *20*, 365704.
(44) Lange, H.; Artemyev, M.; Woggon, U.; Niermann, T.; Thomsen, C. *Phys. Rev. B: Condens. Matter Mater. Phys.* **2008**, *77*, 193303.
(45) Lin, C.; Gong, K.; Kelley, D. F.; Kelley, A. M. *ACS Nano* **2015**, *9*, 8131−8141.
(46) Reiss, P.; Protière, M.; Li, L. *Small* **2009**, *5*, 154−168.
(47) Groeneveld, E.; de Mello Donegá, C. *J. Phys. Chem. C* **2012**, *116*, 16240−16250.
(48) Baranov, A.; Rakovich, Y. P.; Donegan, J.; Perova, T.; Moore, R.; Talapin, D.; Rogach, A.; Masumoto, Y.; Nabiev, I. *Phys. Rev. B: Condens. Matter Mater. Phys.* **2003**, *68*, 165306.
(49) García-Santamaría, F.; Brovelli, S.; Viswanatha, R.; Hollingsworth, J. A.; Htoon, H.; Crooker, S. A.; Klimov, V. I. *Nano Lett.* **2011**, *11*, 687−693.
(50) Chernikov, A.; Bornwasser, V.; Koch, M.; Chatterjee, S.; Böttge, C.; Feldtmann, T.; Kira, M.; Koch, S.; Wassner, T.; Lautenschläger, S.; Meyer, B.; Eickhoff, M. *Phys. Rev. B: Condens. Matter Mater. Phys.* **2012**, *85*, 035201.
(51) Tessier, M.; Mahler, B.; Nadal, B.; Heuclin, H.; Pedetti, S.; Dubertret, B. *Nano Lett.* **2013**, *13*, 3321−3328.
(52) Jiang, Z.-J.; Kelley, D. F. *Nano Lett.* **2011**, *11*, 4067−4073.
(53) Lovingood, D. D.; Achey, R.; Paravastu, A. K.; Strouse, G. F. *J. Am. Chem. Soc.* **2010**, *132*, 3344−3354.
(54) Zhang, J.-Y.; Wang, X.-Y.; Xiao, M.; Qu, L.; Peng, X. *Appl. Phys. Lett.* **2002**, *81*, 2076−2078.
(55) Qu, L.; Peng, X. *J. Am. Chem. Soc.* **2002**, *124*, 2049−2055.
(56) Frederick, M. T.; Amin, V. A.; Cass, L. C.; Weiss, E. A. *Nano Lett.* **2011**, *11*, 5455−5460.
(57) Fernée, M. J.; Tamarat, P.; Lounis, B. *J. Phys. Chem. Lett.* **2013**, *4*, 609−618.
(58) Louyer, Y.; Biadala, L.; Tamarat, P.; Lounis, B. *Appl. Phys. Lett.* **2010**, *96*, 203111.
(59) Rosenthal, S. J.; McBride, J.; Pennycook, S. J.; Feldman, L. C. *Surf. Sci. Rep.* **2007**, *62*, 111−157.
(60) Takagahara, T. *Phys. Rev. Lett.* **1993**, *71*, 3577.
(61) Shim, M.; Guyot-Sionnest, P. *J. Chem. Phys.* **1999**, *111*, 6955−6964.
(62) Rabani, E. *J. Chem. Phys.* **2001**, *115*, 1493−1497.
(63) Li, L.-s.; Alivisatos, A. P. *Phys. Rev. Lett.* **2003**, *90*, 097402.
(64) Shanbhag, S.; Kotov, N. A. *J. Phys. Chem. B* **2006**, *110*, 12211−12217.
(65) Alivisatos, A. P. *J. Phys. Chem.* **1996**, *100*, 13226−13239.
(66) Müller, J.; Lupton, J. M.; Rogach, A. L.; Feldmann, J.; Talapin, D. V.; Weller, H. *Phys. Rev. B: Condens. Matter Mater. Phys.* **2005**, *72*, 205339.
(67) Gómez, D. E.; van Embden, J.; Mulvaney, P. *Appl. Phys. Lett.* **2006**, *88*, 154106.
(68) Cho, K.-S.; Talapin, D. V.; Gaschler, W.; Murray, C. B. *J. Am. Chem. Soc.* **2005**, *127*, 7140−7147.
(69) Kortschot, R.; Van Rijssel, J.; van Dijk-Moes, R.; Erné, B. *J. Phys. Chem. C* **2014**, *118*, 7185−7194.
(70) Peterson, J. J.; Krauss, T. D. *Nano Lett.* **2006**, *6*, 510−514.
(71) Fernée, M. J.; Sinito, C.; Tamarat, P.; Lounis, B. *Nano Lett.* **2014**, *14*, 4480−4485.
(72) Sinito, C.; Fernée, M. J.; Goupalov, S. V.; Mulvaney, P.; Tamarat, P.; Lounis, B. *ACS Nano* **2014**, *8*, 11651−11656.
(73) Ithurria, S.; Bousquet, G.; Dubertret, B. *J. Am. Chem. Soc.* **2011**, *133*, 3070−3077.
(74) Tessier, M. D.; Javaux, C.; Maksimovic, I.; Loriette, V.; Dubertret, B. *ACS Nano* **2012**, *6*, 6751−6758.
(75) Achtstein, A. W.; Schliwa, A.; Prudnikau, A.; Hardzei, M.; Artemyev, M. V.; Thomsen, C.; Woggon, U. *Nano Lett.* **2012**, *12*, 3151−3157.
(76) Ithurria, S.; Tessier, M.; Mahler, B.; Lobo, R.; Dubertret, B.; Efros, A. L. *Nat. Mater.* **2011**, *10*, 936−941.

DOI: 10.1021/acs.nanolett.5b03790
Nano Lett. 2016, 16, 289−296